

Dr. James Woodworth, NASA Postdoctoral Program
 Dr. Richard Baldwin NASA Postdoctoral Program Mentor
 Electrochemistry Branch, NASA Glenn Research Center
 William Bennett, Electrochemistry Branch, NASA Glenn Research Center

Abstract

A variety of materials are under investigation for use as anode materials in lithium-ion batteries, of which, the most promising are those containing silicon.¹⁰ One such material is a composite formed via the dispersion of silicon in a resorcinol-formaldehyde (RF) gel followed by pyrolysis. Two silicon-carbon composite materials, carbon microspheres and nanofoams produced from nano-phase silicon impregnated RF gel precursors have been synthesized and investigated. Carbon microspheres are produced by forming the silicon-containing RF gel into microspheres whereas carbon nanofoams are produced by impregnating carbon fiber paper with the silicon containing RF gel to create a free standing electrode.^{1-4,9} Both materials have demonstrated their ability to function as anodes and utilize the silicon present in the material. Stable reversible capacities above 400 mAh/g for the bulk material and above 1000 mAh/g of Si have been observed.

Introduction

The National Aeronautics and Space Administration (NASA) has embarked upon a number of near and far term missions which require advanced energy storage systems. These energy storage systems must be safe, human rated, have high specific energies (Wh/kg), high energy densities (Wh/l), high reliability, long cycle life, low power fade over the life of the battery and the ability to perform in a variety of unique environments. The Exploration Technology Development Program (ETDP) via the Energy Storage Project supported the development of advanced lithium ion (Li-ion) cells which possess many of the required attributes.

Central to the development of advanced lithium ion batteries is the development of advanced anode materials (figures 1 and 2). Current technologies are centered around graphitic anode materials which have a theoretical capacity of 372 mAh/g. One of the new materials being investigated is silicon which has a theoretical capacity of 4200 mAh/g. However, pure silicon suffers from a 400% lattice volume expansion upon insertion of the lithium ions, resulting in large irreversible capacity loss, cracking of the material, and eventual failure of the anode.¹⁰

One approach to ameliorating the expansion issues associated with silicon is to form a silicon-carbon composite. One such composite material is formed via the dispersion of silicon in a resorcinol-formaldehyde (RF) gel followed by pyrolysis. The premise behind the RF gel silicon composite is that the gel will form a flexible, porous, carbon matrix capable of absorbing the large volume expansion of the silicon upon lithiation thereby maintaining electrical contact between particles and the current collector. The carbon matrix will also prevent direct electrolyte contact with the silicon.^{12,9} Unlike a variety of other approaches, which use complicated expensive techniques such as chemical vapor deposition, this technique makes use of traditional cost-effective laboratory techniques.

Two materials, carbon microspheres (figures 3-4) and carbon nanofoam (figures 7-8), produced from nano-phase silicon impregnated RF gel precursors have been synthesized and investigated. In the first approach the silicon containing RF gel is formed into microspheres (carbon microspheres).^{12,9} In the second approach, carbon paper is impregnated with the silicon containing RF gel to create a free standing electrode (carbon nanofoam).^{3,4,9} which, if successful, would eliminate the need for a current collector. The elimination of the current collector would result in the reduction of mass and an increase in the specific energy compared to cells with traditional coated anode materials (figure 2, table 1).

Objective

The objective of this research project is to develop a silicon-carbon composite anode material with a threshold specific capacity of 600 mAh/g and a goal of 1000 mAh/g as outlined by the Exploration and Technology Development Program Energy Storage Project. It should be noted that the specific energy requirements are expressed for a traditional coated electrode that utilizes a copper current collector.

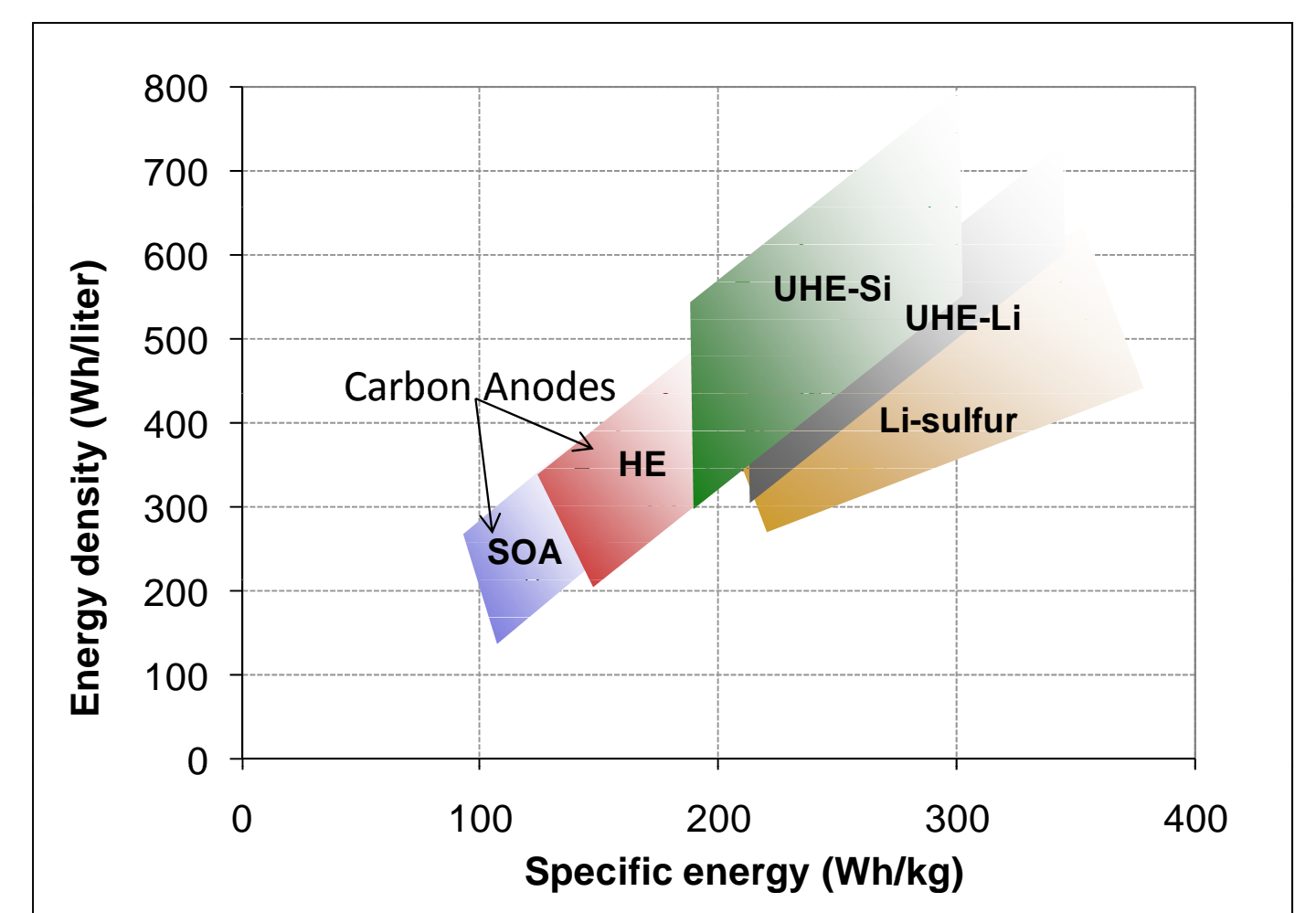
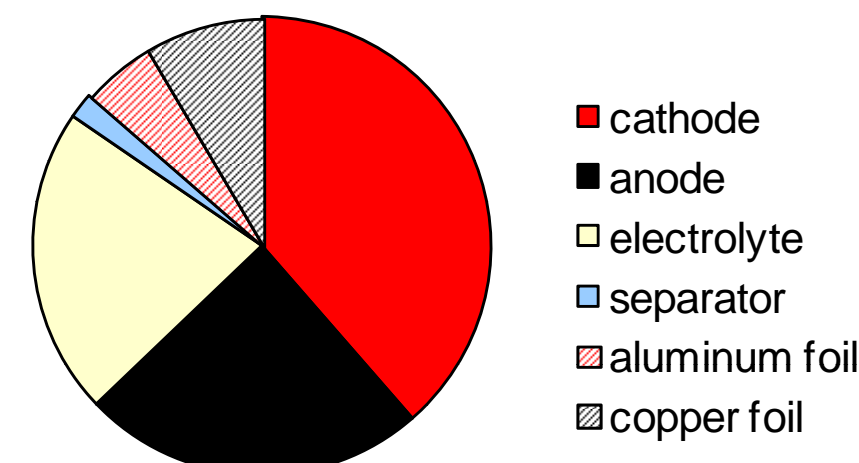


Figure 1. Estimates for cell specific energy and energy density

Figure 2
 Estimates for component weight fraction in 30 Ah cell. Mass of the anode coating represents approximately 24% of total mass. Mass of the copper foil current collector represents approximately 8% of mass.



Approach 1: Carbon Gel Microsphere Anodes

Synthesis^{1,2,7,9}

- Resorcinol-formaldehyde gels containing 50 nm silicon were formed
- Pyrolyzed at 1000° in argon

Cell Construction and Electrochemical Cycling

- Carbon microspheres were slurried with NaCMC and cast with 0.005" film onto copper foil
- Half cells were constructed in the form of coin cells using metallic lithium as the counter electrode
- Electrolyte: 1M LiPF₆ 1:1:1 ethylene carbonate, diethyl carbonate and dimethyl carbonate
- Cells were formed at a rate of C/10 for three cycles
- Cycling was performed at C/10 charge and discharge for 12-15 cycles followed by 5 cycles with a charge rate of C/10 and a discharge rate of C/5
- Cells were cycled at room temperature

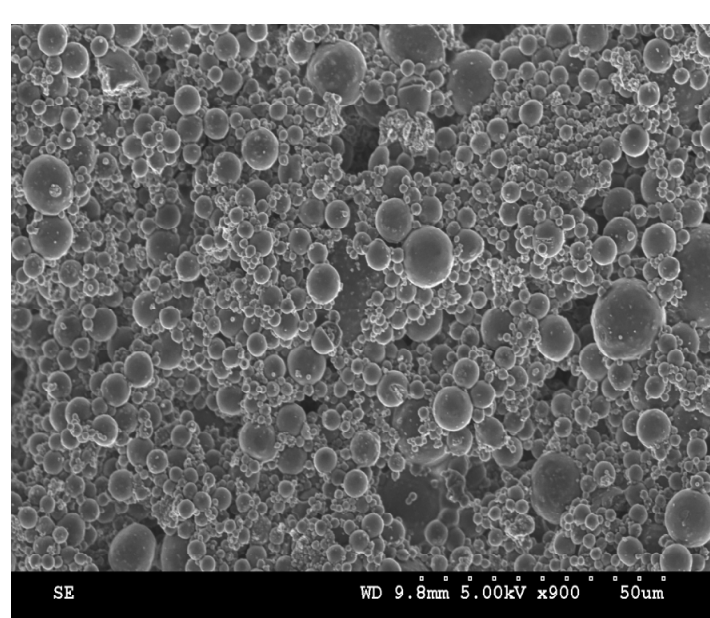


Figure 3 Scanning electron micrograph of cast electrode composed of carbon microspheres containing nano-silicon before cycling

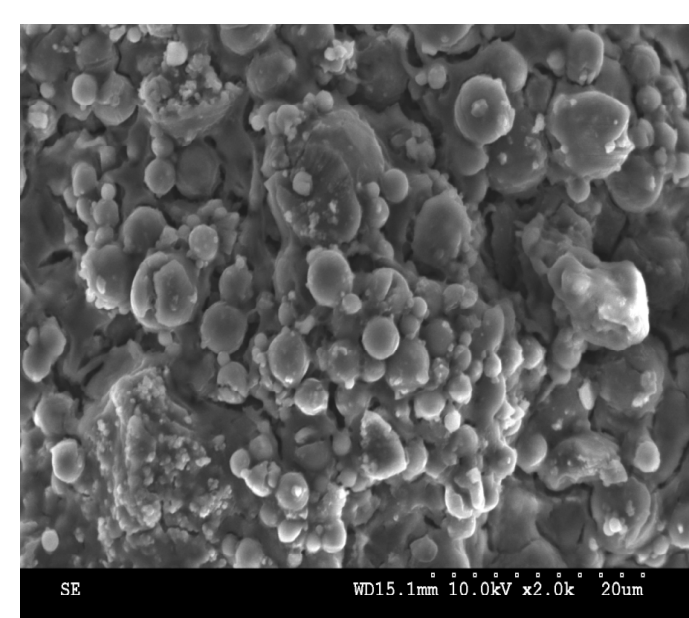


Figure 4 Scanning electron micrograph of cast electrode composed of carbon microspheres containing nano-silicon after cycling

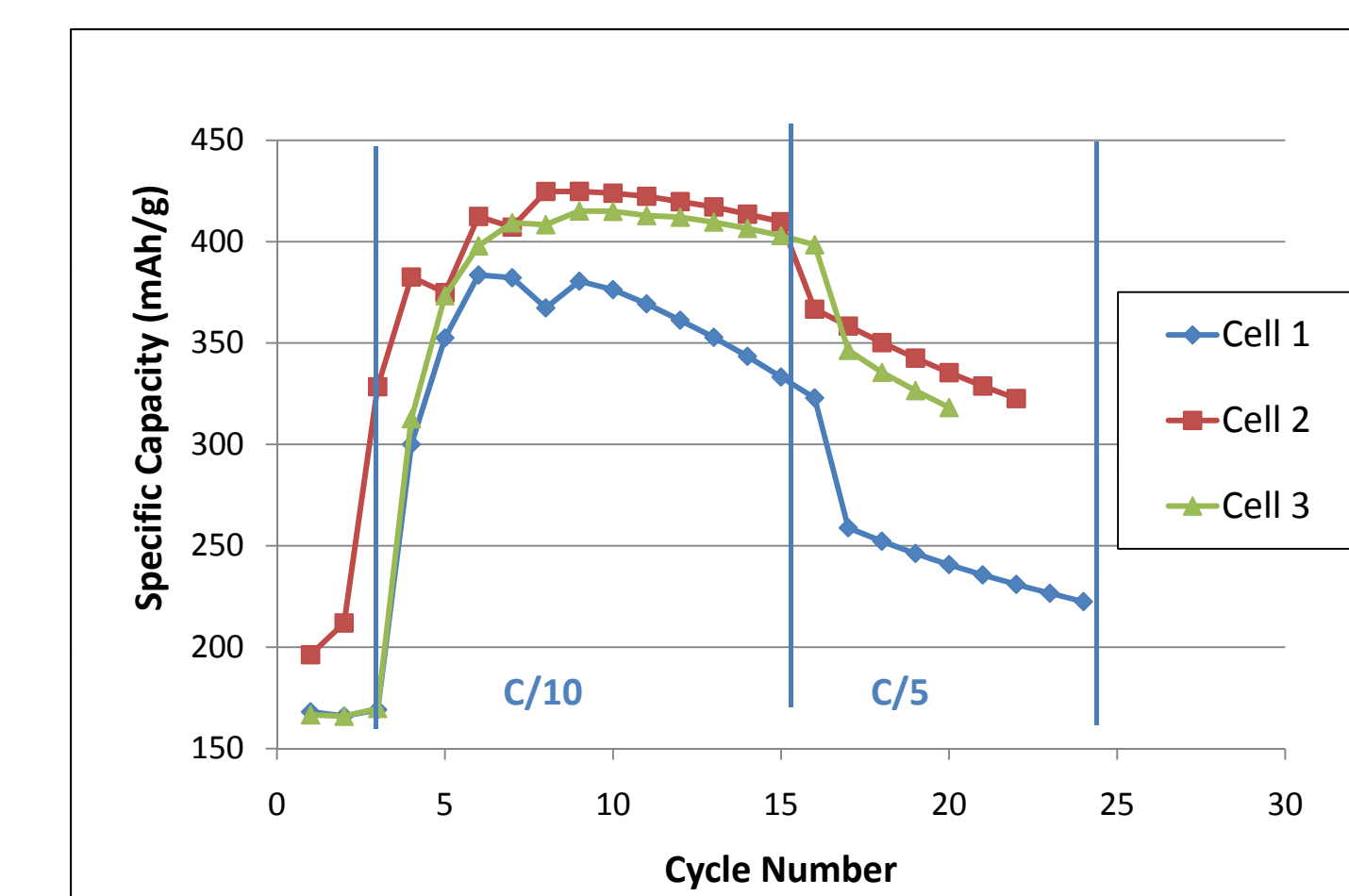


Figure 5 Specific capacity as a function of cycling for cells containing carbon-silicon microsphere anode material

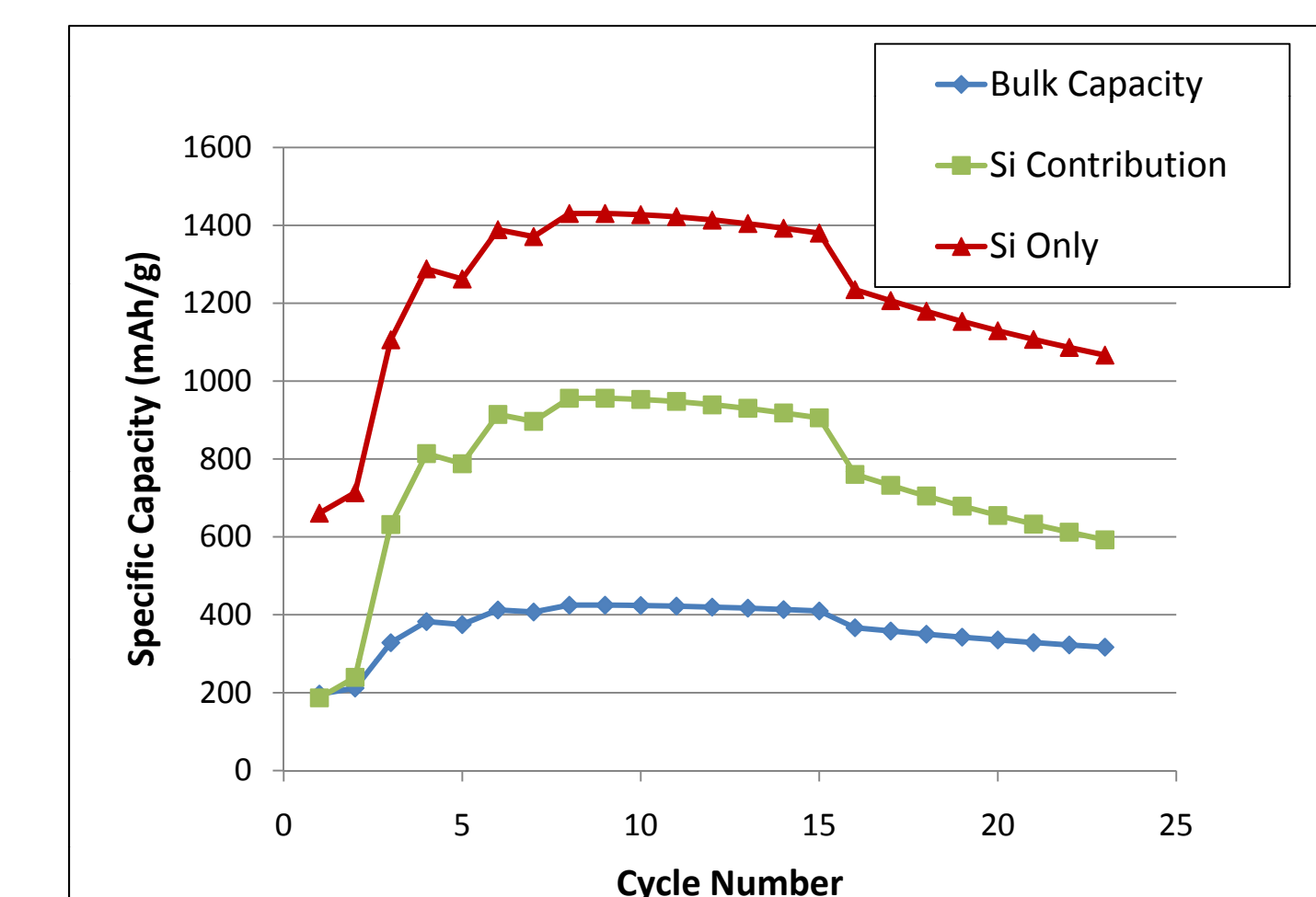


Figure 6 Specific capacity as a function of cycle number for cell 2 in fig. 4 showing capacities for the bulk material, the Si contribution and the capacity based on Si being the only active material

Results for The Silicon-Carbon Microspheres

- Integrity and Spherical morphology are maintained after cycling (figures 3-4) Indicating that the material is capable of buffering the large volume changes of the silicon
- Exhibits unusual increase in capacity with cycling (figure 5)
 - Low capacity (150-200 mAh/g) for first several cycles
 - Capacity suddenly and drastically increases
- Demonstrated ability to utilize the silicon (figure 6)
- Low capacity fade
- First cycle irreversible capacity loss of 50% of the maximum capacity
- Coulombic efficiency of approximately 96% (desired values exceed 99%)

Approach 2 : Carbon Nanofoam Anodes

Significance

- Composed of 100% active material (carbon and silicon)
- Free standing electrode that does not require the use of a copper current collector
 - Could significantly reduce cell mass
 - Effective specific capacity on the electrode level would be higher than for traditional coated electrodes (table 1)

Synthesis^{1,2,7,9}

- Free standing carbon nanofoam anode was produced from carbon paper impregnated with resorcinol-formaldehyde gel containing 50 nm silicon particles
- Pyrolyzed at 1000° C in argon

Cell Construction and Electrochemical Cycling

- Anodes were constructed via two methods
 - Nanofoam material was placed on copper foil current collectors the same size as the anode material (used only for preliminary tests)
 - A nickel tab is spot-welded onto the corner of the nanofoam material (used on most tests)
- Half cells were constructed in the form of pouch cells using metallic lithium as the counter electrode
- Electrolyte: 1M LiPF₆ 1:1:1 ethylene carbonate, diethyl carbonate and dimethyl carbonate
- Cells were formed at a rate of approximately C/5 for 5 cycles then cycled at C/20 for the remaining cycles reported
- Cycled at room temperature

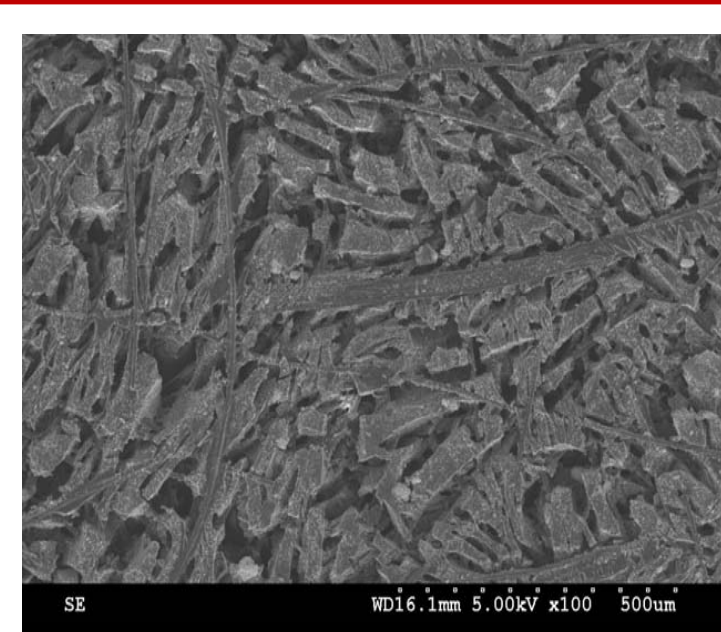


Figure 7 Scanning electron micrograph of carbon nanofoam containing nano-silicon as synthesized



Figure 8 Free standing carbon-silicon nanofoam anode

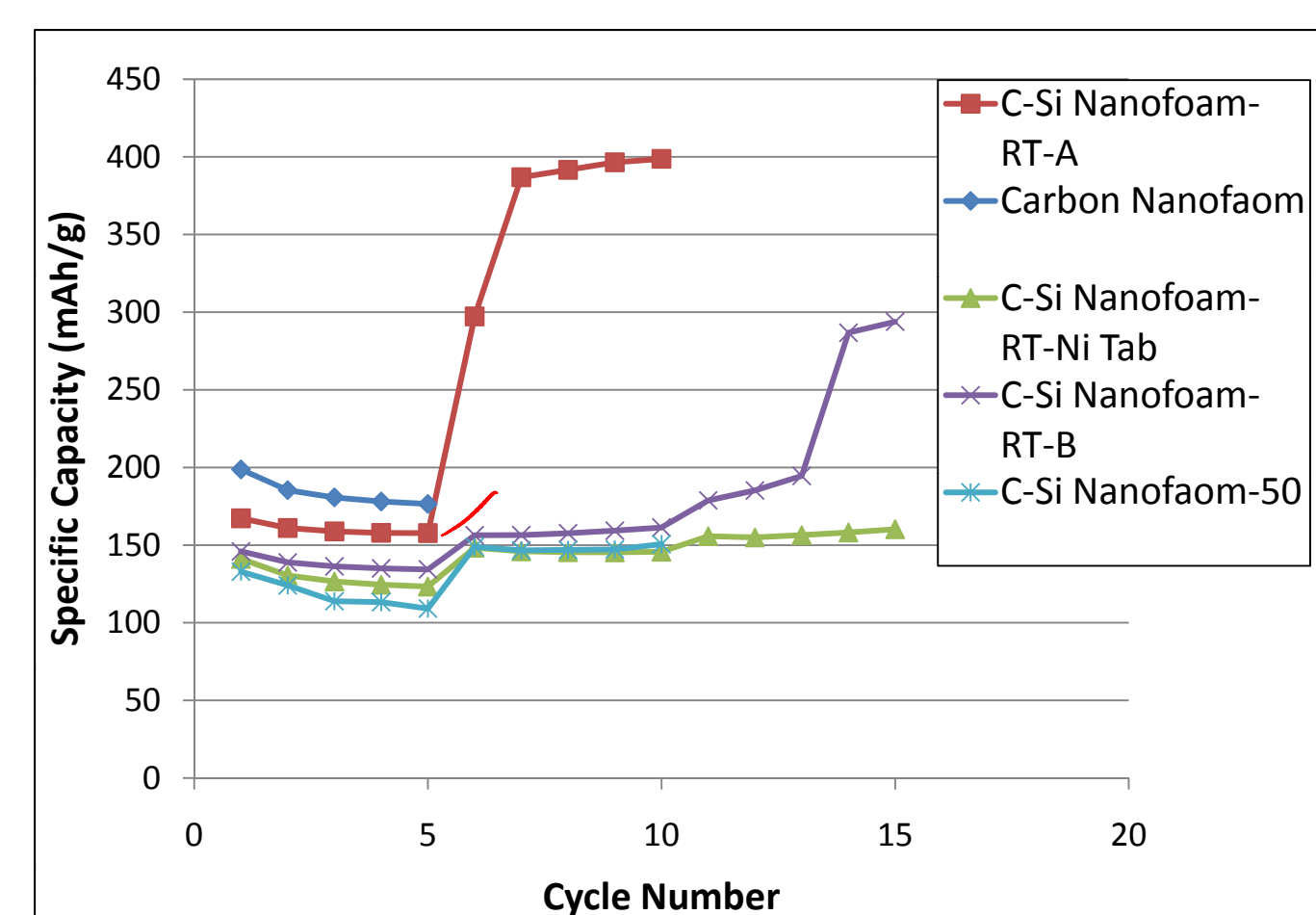


Figure 9 Specific capacity as a function of cycle number for carbon-silicon (C-Si) nanofoam anode material (RT=cured at room temperature (50)=cured at 50°C, (Ni Tab) = sample with a nickel tab attached without a copper foil current collector

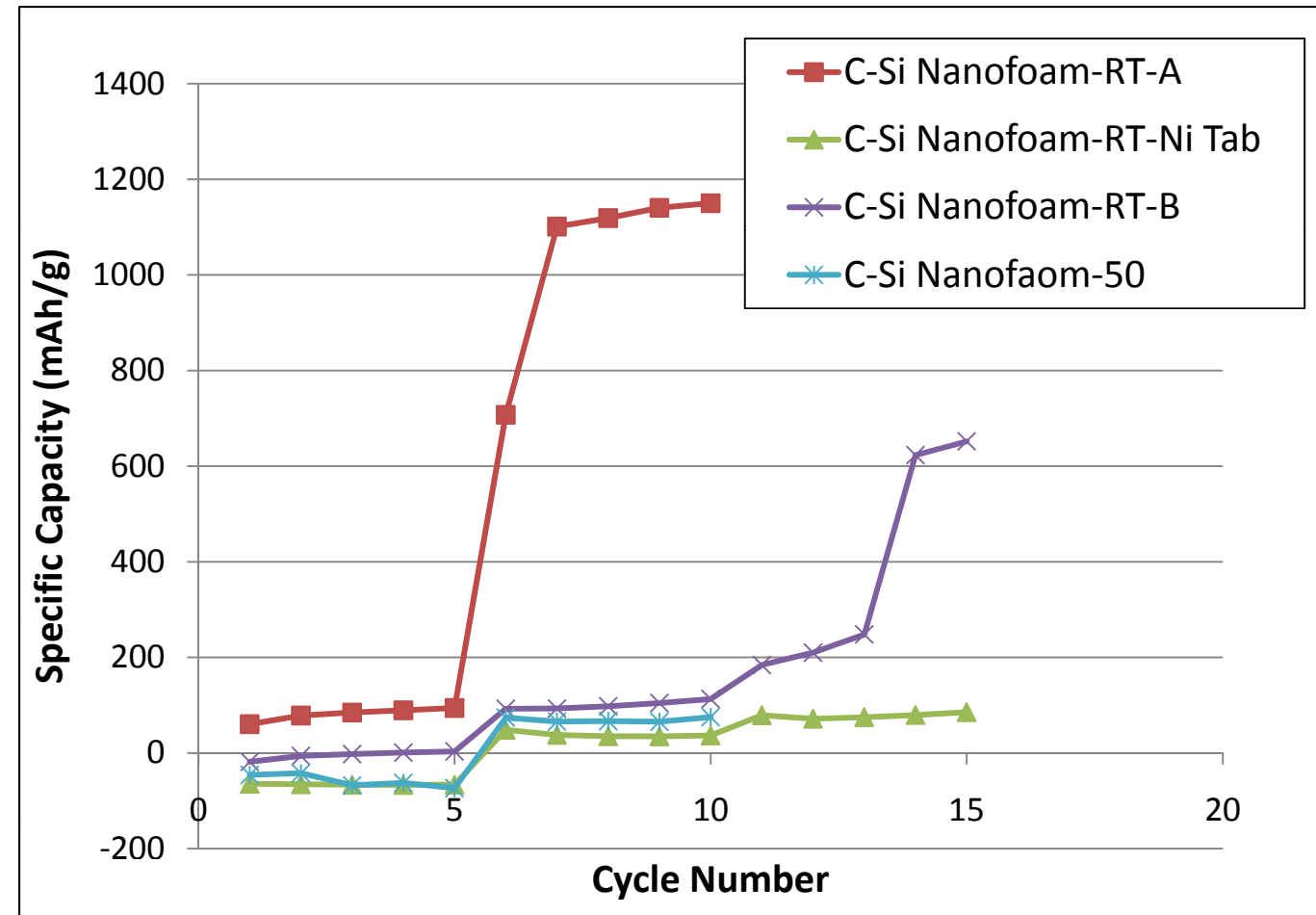


Figure 10 The contribution of silicon to the specific capacity as a function of cycle number for carbon-silicon (C-Si) nanofoam anode material (RT=cured at room temperature (50)=cured at 50°C, (Ni Tab) = sample with a nickel tab attached without a copper foil current collector

Electrode	mAh/g Active Material	mAh/g Electrode
Nanofoam	500	500
Graphite With Cu	350	170
Si With Cu	1000	312

Table 1 Theoretical specific capacities at the active material and electrode levels (Cu=copper current collector)

Initial Results for The Silicon-Carbon Nanofoam

- Materials were shown to intercalate and de-intercalate lithium
- Electrodes identified as C-Si nanofoam RT-A and RT-B showed improving performance with cycling with final capacities of approximately 400 mAh/g and 275 mAh/g respectively at the electrode level
- Material has the ability to function as an anode and utilize the capacity of the silicon (figure 10)
- Electrode with the spot welded nickel tab performed comparably with electrodes which utilized a-copper foil current collector (figures 9 and 10)
 - Current collectors may not be necessary when using this material
 - Significant reduction in electrode mass
- The absence of the current collector significantly reduces the mass of the electrode thereby increasing specific energy at the electrode level when compared to traditional coated anode materials (figure 2, table 1)

Analysis of Cycling Characteristics

- Both the microspheres and the nanofoam anode materials showed low initial capacity followed by a sudden and drastic increase in capacity after several cycles.
- The increase in capacity occurred after the cell had undergone an extended taper charge in which the cell was held at a low voltage (about 10-15mV) vs. Li for an extended period of time (figure 11 a).
- After the extended taper charge and during cycles with improved capacity a shoulder, indicative of de-lithiation of silicon, appeared in the voltage vs. time discharge (de-lithiation) curve (figure 12a)¹²
- dQ/dV analysis revealed that the increase in capacity correlates with the formation of highly lithiated amorphous silicon phases.¹²
- Microsphere cell 1 dQ/dV curves for cycles 1-3 are dominated by characteristics associated with the intercalation of carbon by lithium. After cycle 4 in which the cell undergoes an extended taper charge at low voltage (figure 11a) the silicon de-lithiation peak at 0.4 V becomes more pronounced with each successive cycle (figure 13) and features associated with the lithiation of amorphous silicon appear (figure 13b,c).¹²
- Speculative mechanism to explain the unusual cycling characteristics (figure 14)
 - During the first few cycles, the lithium is only able to access the carbon which surrounds the silicon and perhaps the small percentage of silicon located close to the surface
 - Carbon becomes fully lithiated which, in turn, allows for the lithiation of silicon surrounded by the carbon
 - Diffusion pathways are established which allow for more efficient lithiation and de-lithiation of the silicon

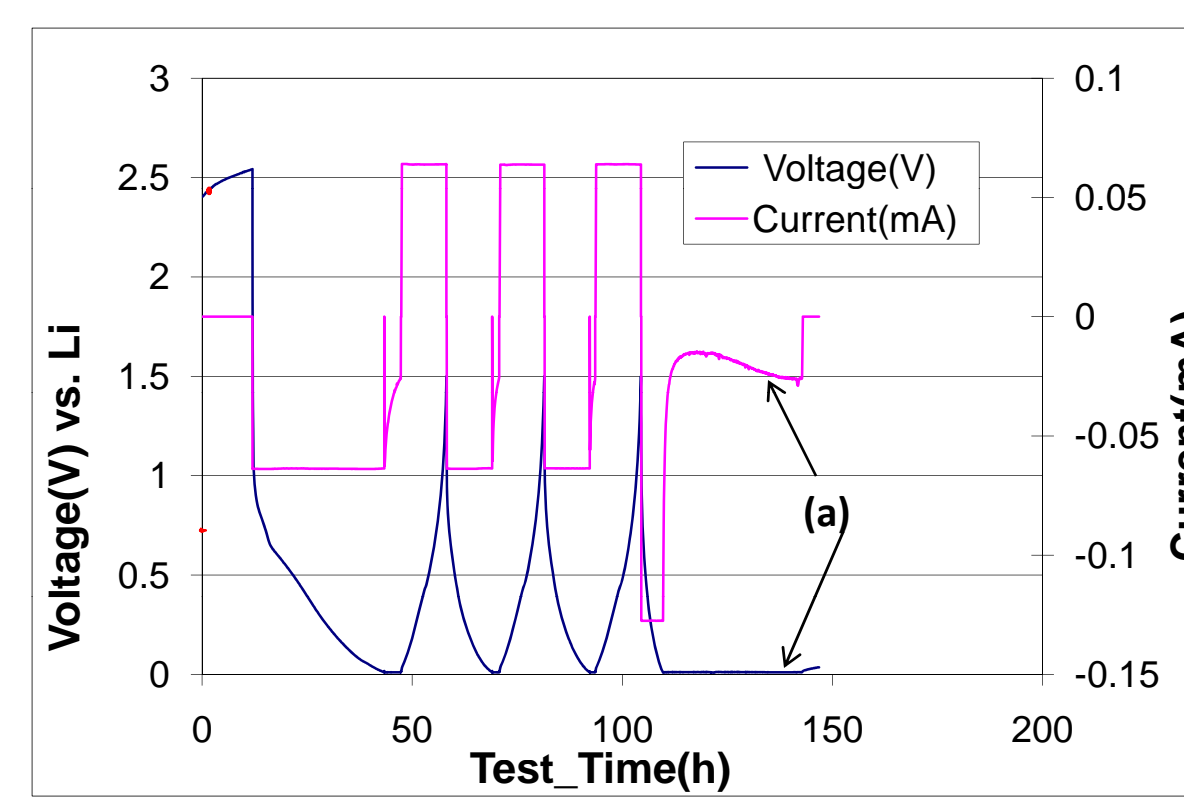


Figure 11 Voltage and Current vs. Test Time for cycles 1-3 of carbon-silicon microsphere cell 1 (a) extended taper charge observed prior to large increase in specific capacity of anode.

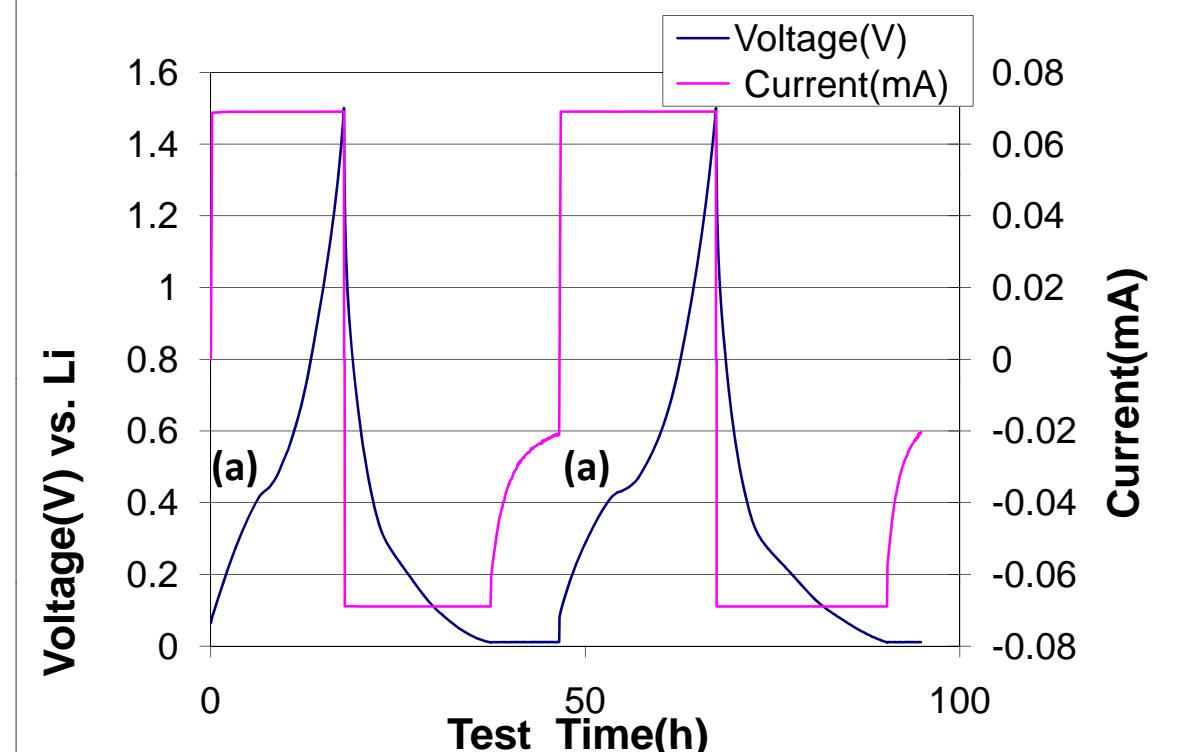


Figure 12 Voltage and Current vs. Test Time for cycles 4-5 of carbon-silicon microsphere cell 1. (a) shoulders indicative of de-lithiation of silicon

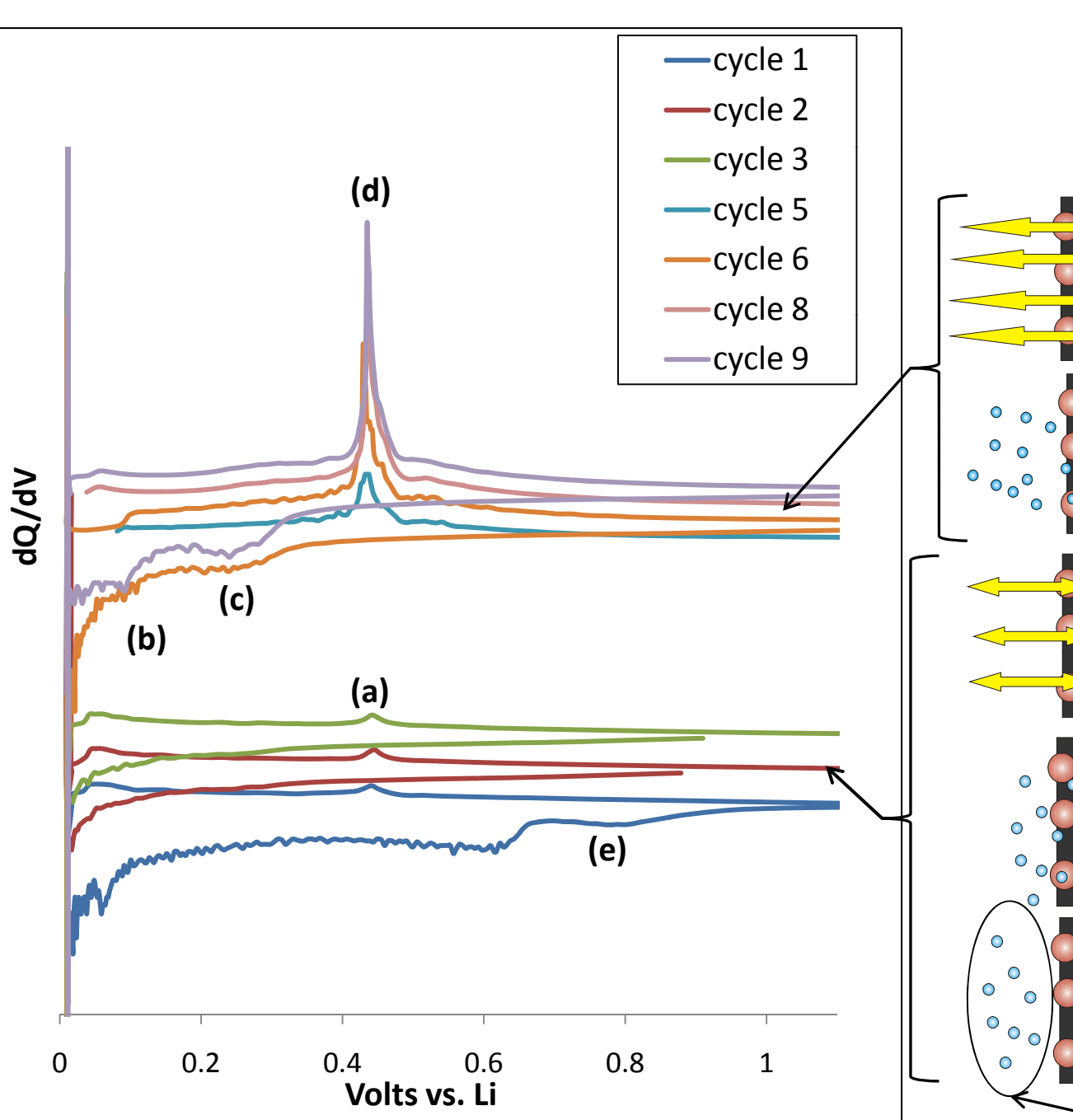


Figure 13 dQ/dV analysis of carbon-silicon microsphere cell 1 (a) and (d) de-lithiation of silicon¹² (b) and (c) lithiation of silicon¹² (e) SEI formation

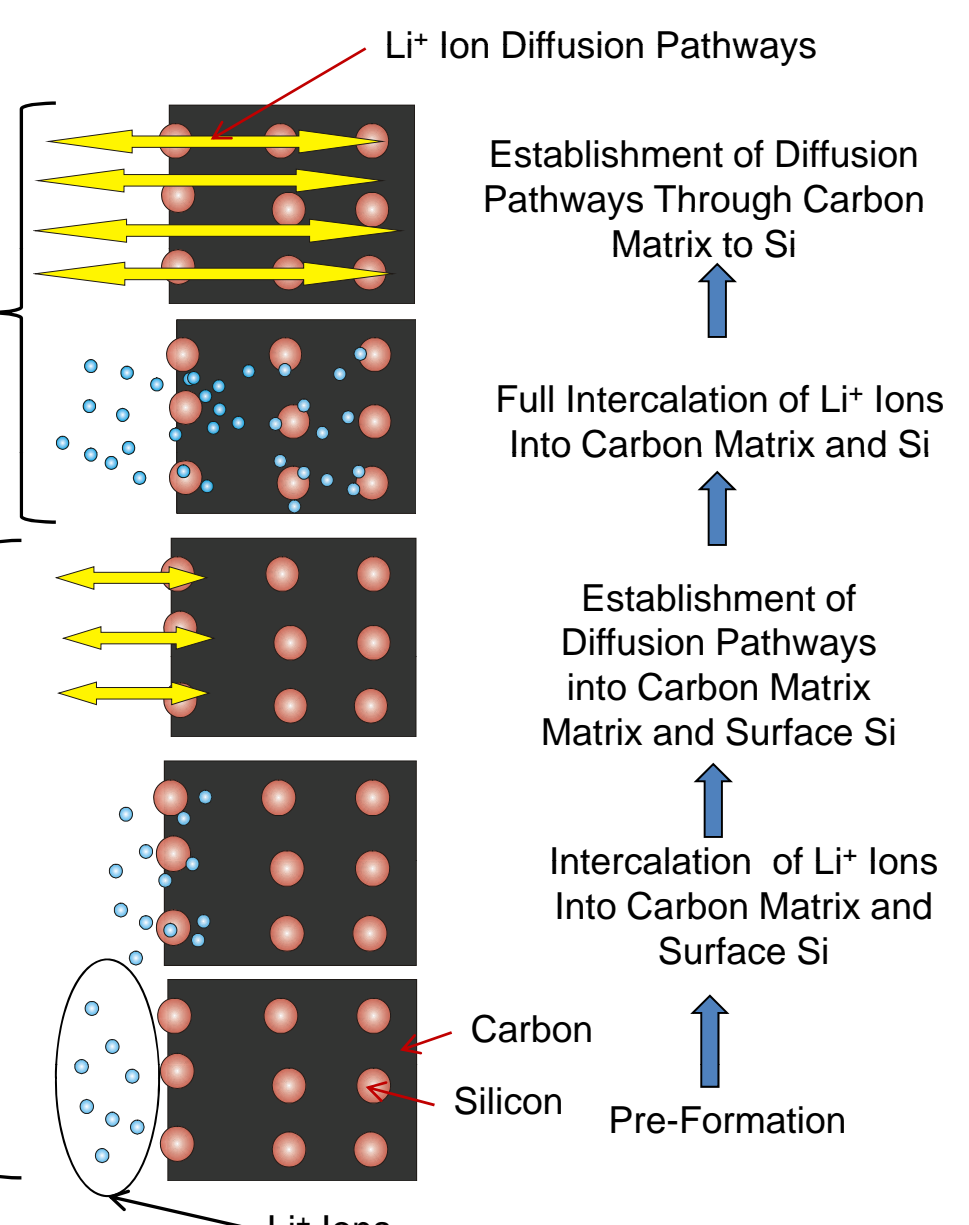


Figure 14 Speculative mechanism explaining the increase in specific capacity with continued cycling

New Approaches for Silicon-Carbon Nanofoam

- Add graphite to resorcinol formaldehyde gel to improve conductivity
- Coat the anode with a conductive binder composed of polyaniline doped with LiPF₆¹¹
- Improve initial capacity and promote faster lithiation of the silicon by developing a new formation/cycling procedure in which the cell is formed very slowly and the taper charge is replaced with a low current constant current step
- Use only spot welded nickel tabs and no copper current collector

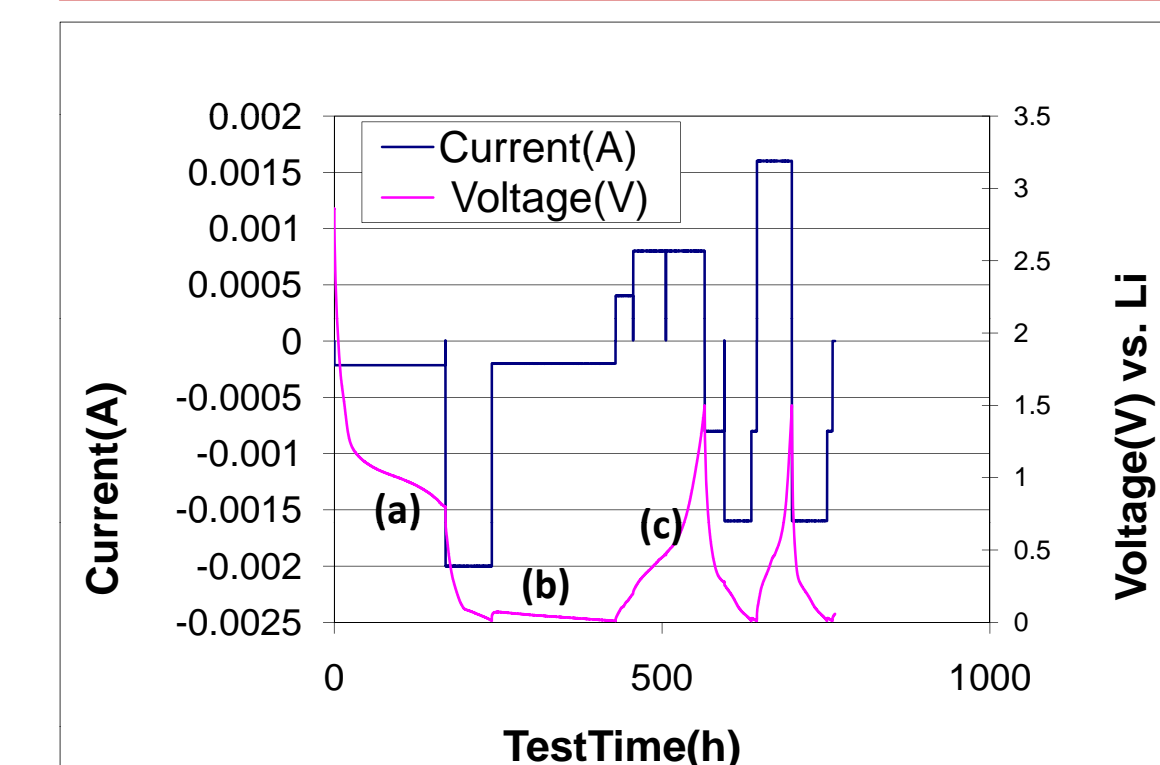


Figure 15 Voltage and Current vs. Test Time for cycles 1 and 2 of the carbon-silicon-graphite nanofoam anode. (a) slow first insertion, (b) low current (C/100) constant current step to a cutoff voltage of 10 mV, (c) shoulders indicative of de-lithiation of silicon

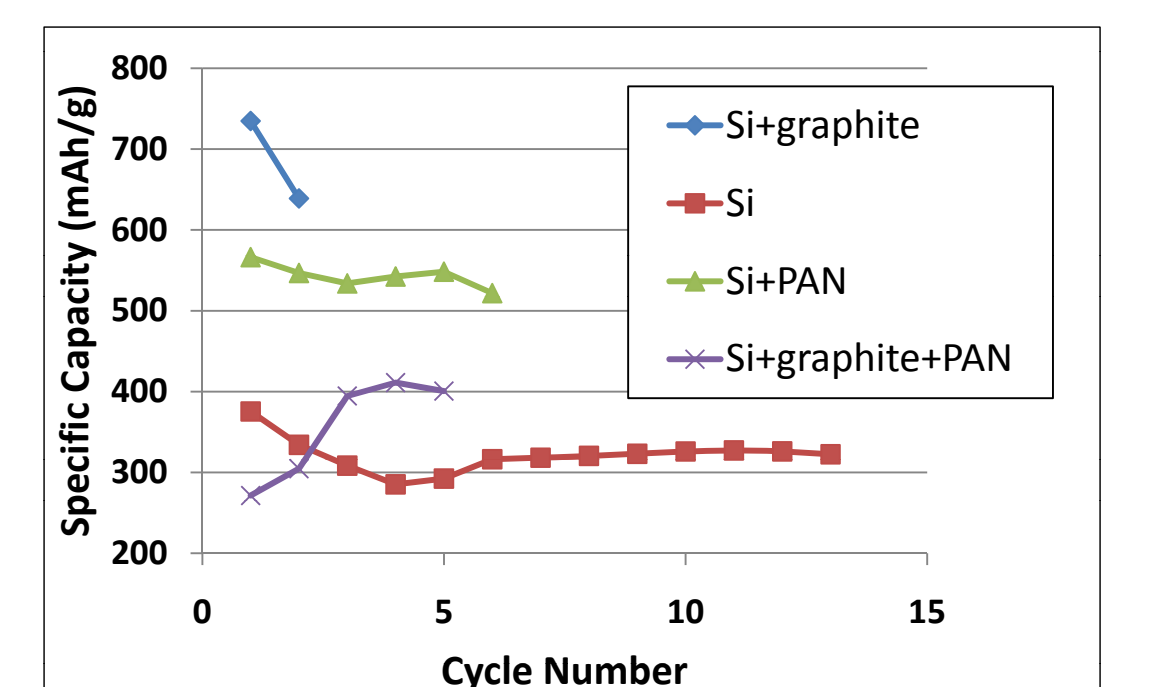


Figure 16 Specific capacity as a function of cycle number for carbon-silicon nanofoam anode material (PAN=coated with polyaniline doped with LiPF₆)

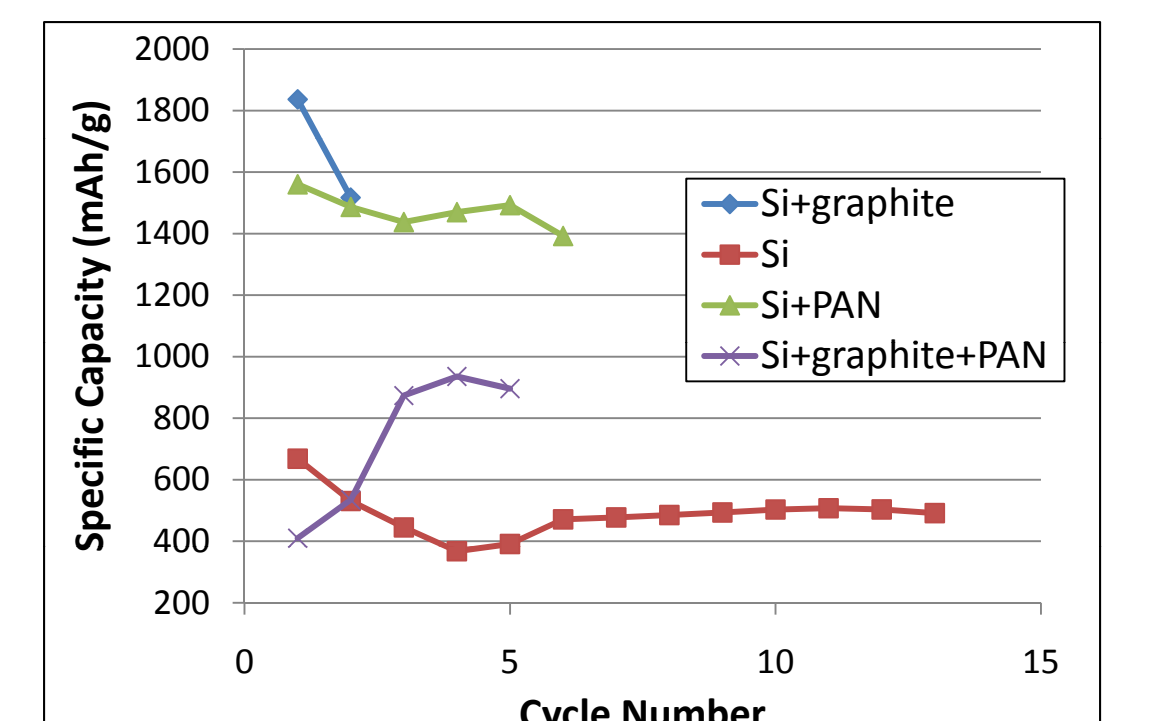


Figure 17 The contribution of silicon to the specific capacity as a function of cycle number for carbon-silicon nanofoam anode material (PAN=coated with polyaniline doped with LiPF₆)

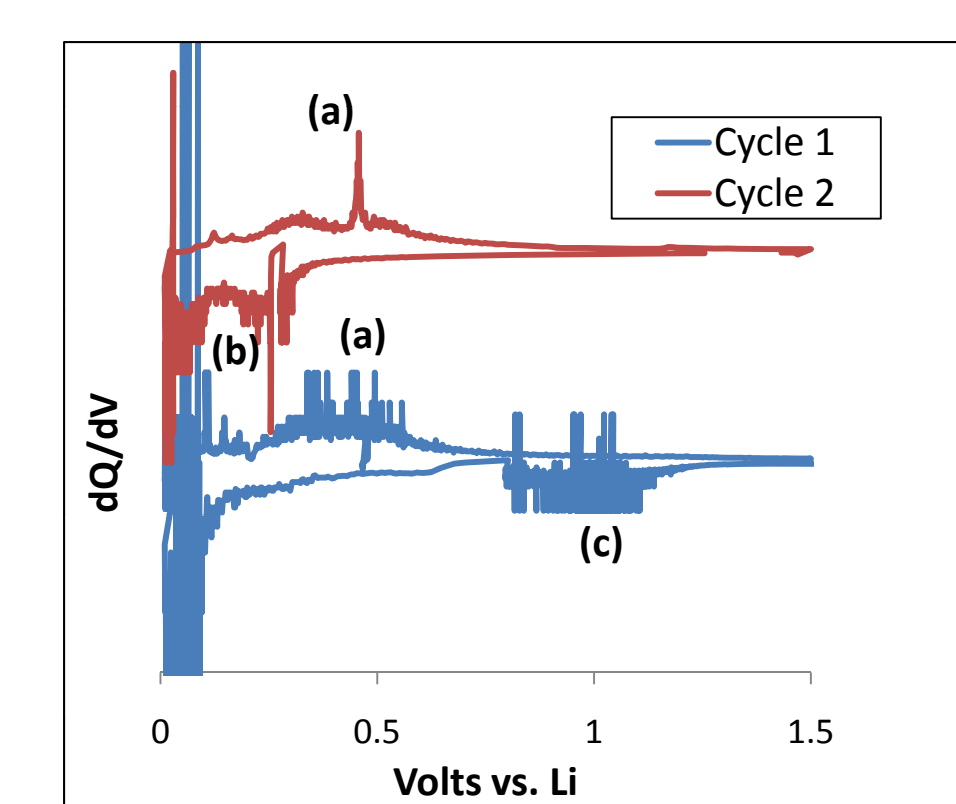


Figure 18 dQ/dV analysis of the first two cycles of the silicon-carbon-graphite nanofoam anode. (a) de-lithiation of silicon¹², (b) lithiation of silicon¹², (c) SEI formation

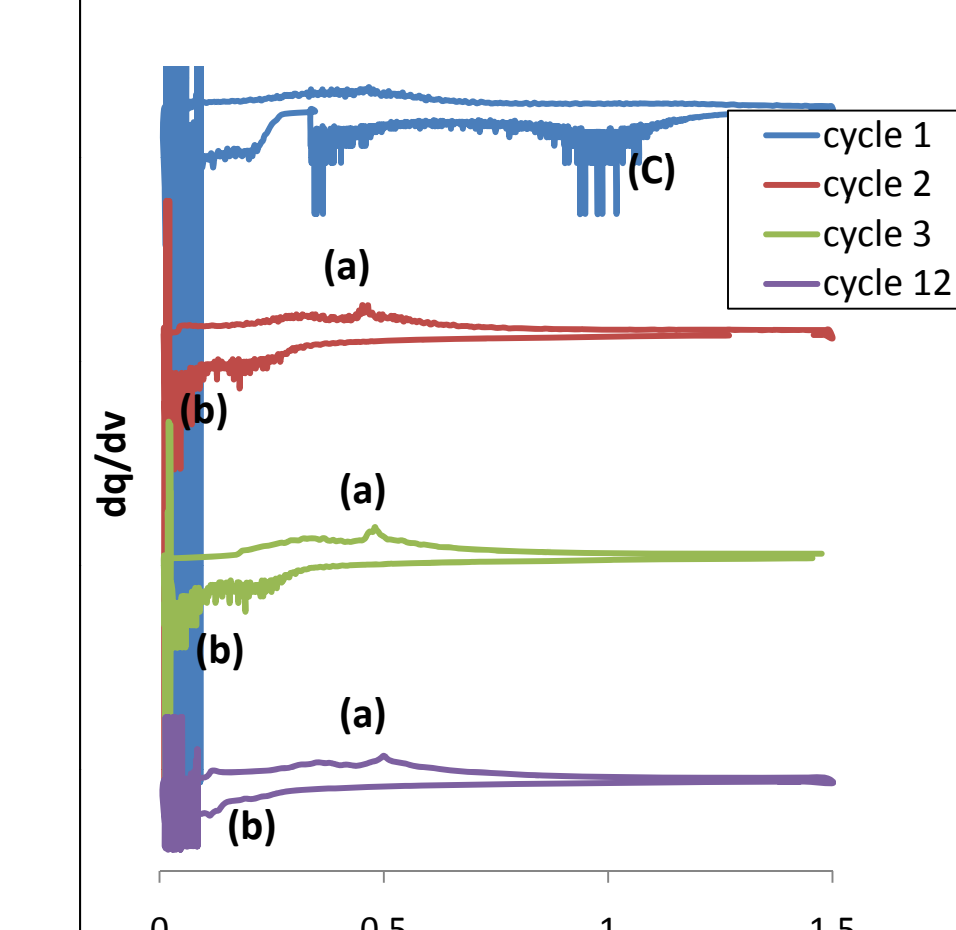


Figure 19 dQ/dV analysis of the silicon-carbon anode. (a) de-lithiation of silicon¹², (b) lithiation of silicon¹², (c) SEI formation

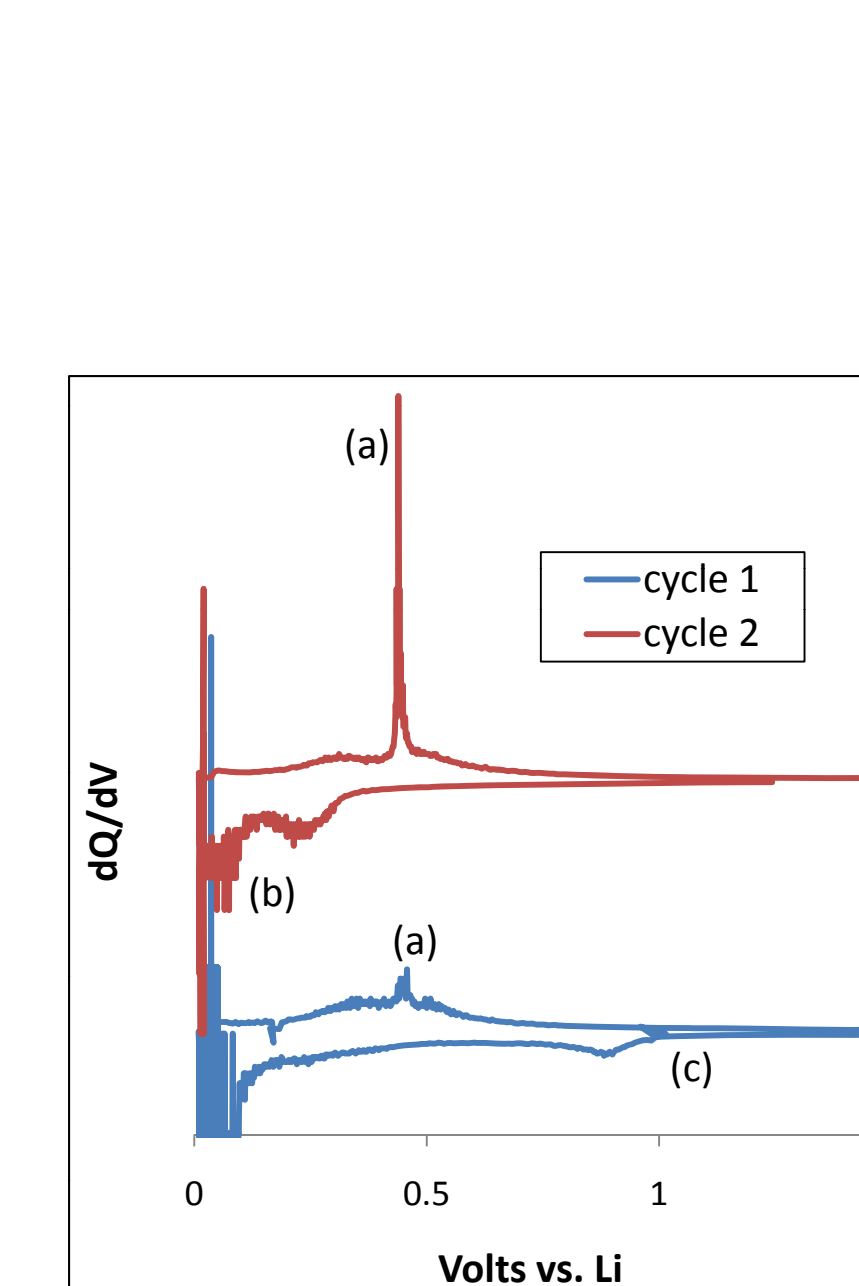


Figure 20 dQ/dV analysis of the first two cycles of the silicon-carbon-nanofoam anode coated with polyaniline doped with LiPF₆. (a) de-lithiation of silicon¹², (b) lithiation of silicon¹², (c) SEI formation

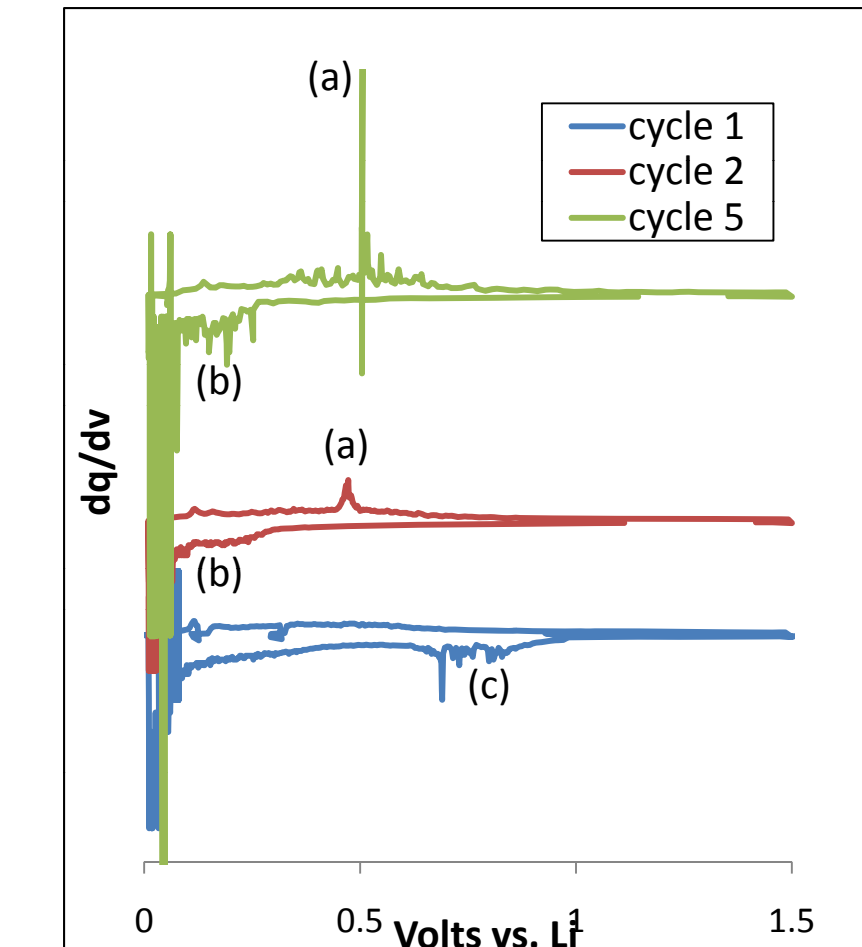


Figure 21 dQ/dV analysis of silicon-carbon-graphite nanofoam anode coated with polyaniline doped with LiPF₆. (a) de-lithiation of silicon¹², (b) lithiation of silicon¹², (c) SEI formation

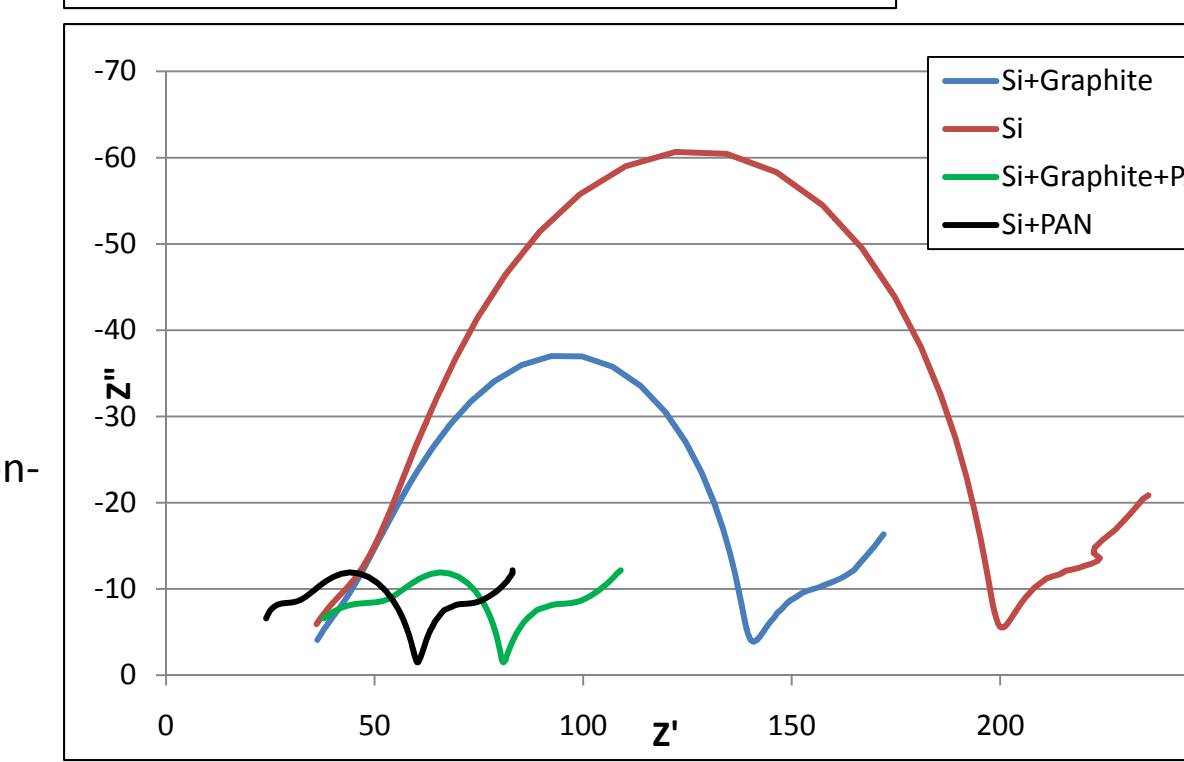


Figure 22 Nyquist plot for carbon-silicon nanofoam anodes

Recent Results for The Silicon-Carbon Nanofoam

- The addition of graphite to the silicon containing carbon nanofoam dramatically increases capacity
- The addition of a coating composed of polyaniline and LiPF₆ to the silicon only carbon nanofoam resulted in a dramatic increase in capacity
- The polyaniline coating appears to have a detrimental effect on the performance of the nanofoam that contains graphite
- The nanofoam containing graphite has a lower impedance than the nanofoam which does not contain graphite (figure 22)
- Samples coated with polyaniline/LiPF₆ show drastically lower impedances than those without the coating (figure 22)
- The presence of graphite in combination with the polyaniline coating resulted in a higher impedance than that of a coated sample not containing graphite (figure 22)
- The features associated with the lithiation and de-lithiation of silicon¹² are more pronounced in the samples that contain graphite or have a polyaniline/LiPF₆ coating (figures 18,20,21 than those that do not (figure 19)
- The implementation of the slow formation cycle and low current constant current step resulted in the lithiation of the silicon within the first cycle and the subsequent improvement in first cycle capacities. This can be observed in the dQ/dV analysis of the nanofoams which shows pronounced formation of features associated with the lithiation and de-lithiation of silicon¹² within the first two cycles (figures 18-21)
- dQ/dV analysis shows that features associated with the formation of an SEI layer appeared only in the first cycle around 1V (feature (c) in figures (18-21).
- First cycle irreversible capacity losses of 100% of the maximum capacity
- Coulombic efficiency of approximately 96%

Conclusions

- Carbon-silicon composite anode materials have been successfully formed from nano-Si containing resorcinol-formaldehyde gel precursors. These materials are in the form of microspheres or monolithic nanofoams. Both materials have demonstrated the ability to function as anodes and utilize the capacity of the silicon present in the material.
- The addition of graphite or a polyaniline/LiPF₆ coating dramatically improves capacity, which can be correlated with an improvement in the utilization of the silicon, and decreases impedance
- The implementation of the slow formation cycle and low current constant current step resulted in the lithiation of the silicon within the first cycle and the subsequent improvement in first cycle capacities.
- Several of these materials meet and/or exceed the EDP threshold value of 600 mAh/g and would likely compare favorably, with regard to specific capacity at the electrode level to conventional coated anode materials
- Though the carbon nanofoam anodes are in an early stage of development and do not yet possess all of the desired performance characteristics, the recent advances in specific capacity of the materials demonstrate significant potential for future development. This is particularly the case since these materials do not require a current collector, which represents approximately 8% of a cell's mass, and therefore would offer additional overall mass savings at the cell level.

Acknowledgements

- This research was supported by an appointment to the NASA Postdoctoral Program at NASA Glenn Research Center administered by Oak Ridge Associated Universities through a contract with NASA funded by the Exploration Technology Development Program, Energy Storage Project
- NASA Glenn Research Center Electrochemistry Branch with special thanks to:
 - Eunice Wong (ASRC)
 - Concha Reid (NASA GRC)
 - Tom Miller (NASA GRC)
 - Dave Yendriga (Sierra Lobo)
 - Marjorie Moats (SGT)
 - Michelle Manzo (Electrochemistry Branch Chief NASA GRC)

References

- Wang, K.; He, X.; Wang, L.; Ren, J.; Jiang, C.; Chunrong, W. *Solid State Ionics* **2007**, *178*, 115-118.
- Hasegawa, T.; Mukai, S. R.; Shirato, Y.; Tamon, H. *Carbon* **2004**, *42*, 2573-2579.
- Long, J. W.; Bourg, M. E.; Wallace, J. M.; Fischer, A. E.; Lytle, J. C.; Pettigrew, K. A.; Barrow, A. J.; Dysart, J. L.; Rolinson, D. R. In *215 Electrochemical Society Meeting* San Francisco CA, 2009.
- Long, J. W., 2009, pp Personal Communication.
- Al-Muhtaseb, Ritter. *Advanced Materials* **2003**, *15*, 101-114
- Yamamoto, Endo, Ohmori, Nakaiwa. *Carbon* **2005**, *43*, 1231-1238.
- Yamamoto, Sugimoto, Suzuki, Mukai, Tamon *Carbon* **2002**, *40*, 1345-1351.
- Hasegawa, T.; Mukai, S. R.; Shirato, Y.; Tamon, H. *Carbon* **2004**, *42*, 2573-2579.
- Wang, G. X.; Ahn, J. H.; Yao, J.; Bewlay, S.; Liu, H. K. *Electrochemistry Communications* **2004**, *6*, 689-692.
- Kasavajula, U.; Wang, C.; Appleby, J. A. *Journal of Power Sources* **2007**, *163*, 1003-1039.
- Liu, Y.; Matsumura, T.; Imanishi, N.; Hirano, A.; Ichiwaka, T.; Takeda, Y. *Electrochemical and Solid State Letters* **2005**, *8*, A599-A602.
- Obrovac, M.N.; Krause, L.J. *Journal of The Electrochemical Society* **2007**, *154*, A103-A108